

# Design and Fabrication of PERC-Like CdTe Solar Cells Using Micropatterned Al<sub>2</sub>O<sub>3</sub> Layer

Etee Kawna Roy<sup>1</sup>, Kaden Powell<sup>1</sup>, Chungho Lee<sup>2</sup>, Gang Xiong<sup>2</sup>, and Heayoung Yoon<sup>1</sup>

<sup>1</sup>Department of Electrical and Computer Engineering, University of Utah, Salt Lake City, UT 84112, USA

<sup>2</sup>California Technology Center, First Solar Inc., Santa Clara, CA, USA.

**Abstract**—Recent studies have investigated novel strategies to further improve the limited  $V_{oc}$  of CdTe solar cells via increased carrier lifetime and doping density of CdTe thin films. Among various metal oxides, aluminum oxide (Al<sub>2</sub>O<sub>3</sub>) is a promising passivation candidate, where the negatively charged Al<sub>2</sub>O<sub>3</sub> layer repels the minority carrier in CdTe and Al<sub>2</sub>O<sub>3</sub> provides a chemically passivating interface, increasing the carrier lifetime. Despite the continuing efforts, an optimized back-contact architecture to improve the  $V_{oc}$  while maintaining high  $J_{sc}$  and  $FF$  is still under development. In this work, we report the design, fabrication, and characterization of PERC-like CdTe solar cells, where an Al<sub>2</sub>O<sub>3</sub> passivation layer is patterned using laser-beam lithography. Our process enables reproducible patterning on a rough surface CdTe while maintaining the size of the array in the design. Analysis of CdTe PERC devices (As-doped) shows a notably different  $V_{oc}$  trend compared to  $FF$  and  $J_{sc}$ , independent of the patterned array structures used in this study. The subsurface electronic structure of CdTe and the interplay between carrier selectivity and collection of the patterned Al<sub>2</sub>O<sub>3</sub> could be responsible for the observed PV characteristics.

## I. INTRODUCTION

Thin-film CdTe solar cells are a competitive photovoltaic (PV) technology that can meet the rapidly growing societal demand for energy owing to cost-effective manufacturing and relatively short energy payback time [1, 2]. At a record efficiency of 22.1 %, significant attention has been devoted to further improving the power conversion efficiencies of CdTe-based solar cells [3-5]. An optimized front contact that leads the  $J_{sc}$  over 31 mA/cm<sup>2</sup> and a fill factor (FF) above 79 % were reported [6, 7]. An open-circuit voltage ( $V_{oc}$ ) over 1 V was achieved with As-doped CdTe single crystals. Despite the continuing efforts, high  $V_{oc}$  (> 1 V) has not yet been observed in thin-film polycrystalline CdTe PVs. The underlying physical mechanisms responsible for the  $V_{oc}$  loss are not presently well understood.

Recent studies have demonstrated novel device architectures and passivation strategies to enhance the  $V_{oc}$  via increasing carrier lifetime and doping density of CdTe thin films. Among various metal oxides, Al<sub>2</sub>O<sub>3</sub> is a promising passivation candidate, where the negatively charged Al<sub>2</sub>O<sub>3</sub> layer (fixed charge density of 10<sup>12</sup> ~ 10<sup>13</sup> cm<sup>-2</sup>) could repel the minority carrier (electrons) in CdTe, increasing the carrier lifetime [7, 8]. Previous studies also suggested that Al<sub>2</sub>O<sub>3</sub> could passivate the CdTe surface via chemical reactions during the fabrication processes. This configuration is similar to a passivated emitter and rear contact (PERC) design, frequently used in Si

photovoltaic (PV) technology [9, 10]. An improved  $V_{oc}$  was reported with a conformal Al<sub>2</sub>O<sub>3</sub> (< 5 nm) on CdTe, yet the  $J_{sc}$  and FF suffer from the tunneling barrier [11-18]. On the other hand, Kephart and co-workers used a 20 nm-thick Al<sub>2</sub>O<sub>3</sub> with micropatterning. A remarkably high lifetime ( $\tau_2 > 400$  ns) was measured for double heterostructures, but no consistent improvement of  $V_{oc}$  was observed for the Cu-doped CdTe solar cells [11].

This work reports the design and fabrication of PERC-like CdTe solar cells (CdTe PERC), where the Al<sub>2</sub>O<sub>3</sub> passivation layer is patterned via laser-beam lithography. We optimize the beam dose to polymerize the photoresist on a rough surface CdTe while maintaining the size of the array in the design. We measure the dark and light  $I$ - $V$ s of As-doped CdSeTe PERC having different hole diameters and pitches (i.e., the distance between adjacent holes). Quantitative analysis shows the impact of Al<sub>2</sub>O<sub>3</sub> patterns on  $V_{oc}$  is notably different from other device parameters of  $J_0$ ,  $J_{sc}$ , and  $FF$ . We discuss a similar  $V_{oc}$  trend observed after annealing (70°C for 2.5 hours) of the complete CdTe PERC. Our results indicate the electrically-active Al<sub>2</sub>O<sub>3</sub> patterns, in conjunction with the defect chemistry in CdTe bulk, could play an essential role in determining the  $V_{oc}$  of advanced CdTe-based solar cells.

## II. EXPERIMENT

Figure 1(a) displays a schematic of a CdTe PERC device consisting of a thin-film CdTe solar cell and a patterned Al<sub>2</sub>O<sub>3</sub>. The As-doped CdSeTe/CdTe absorber layer was synthesized on a stack of buffer/TCO [transparent conductive oxide]/glass substrate. A scanning electron microscopy (SEM) image shows a representative Al<sub>2</sub>O<sub>3</sub> hole array on CdTe fabricated in this work (Figure 1b). The same-size individual holes are uniformly

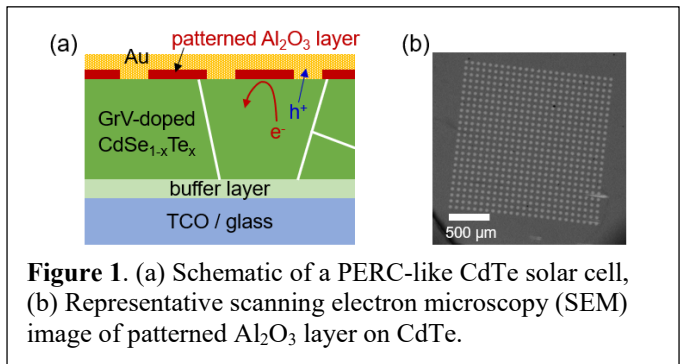
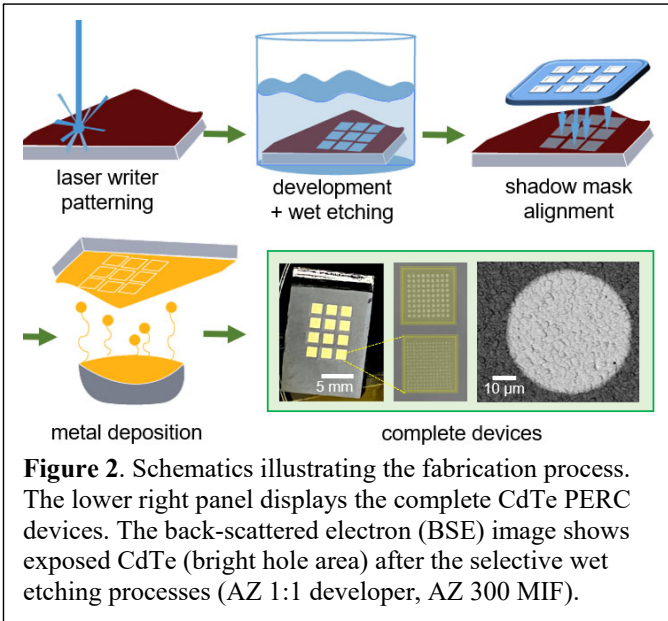


**Figure 1.** (a) Schematic of a PERC-like CdTe solar cell, (b) Representative scanning electron microscopy (SEM) image of patterned Al<sub>2</sub>O<sub>3</sub> layer on CdTe.



distributed in a square pattern across the entire device. This study used three different hole sizes (10  $\mu\text{m}$ , 20  $\mu\text{m}$ , and 40  $\mu\text{m}$ ). The distance between the adjacent holes ranges from 10  $\mu\text{m}$  to 320  $\mu\text{m}$ , introducing different sizes of the exposed CdTe area to metal contact.

Figure 2 illustrates the fabrication procedures to produce patterned  $\text{Al}_2\text{O}_3$  back contacts. As-doped CdSeTe/CdTe solar cells were obtained from First Solar that was coated with a 20 nm  $\text{Al}_2\text{O}_3$  layer. The samples were cleaned with acetone and isopropyl alcohol (IPA), and blown dry with nitrogen ( $\text{N}_2$ ). The samples were baked on a hot plate at 100°C for 60 seconds and cooled down before spin coating of photoresist. A thin layer of positive photoresist (Shipley1813) was coated on the sample at a spin speed of 3,000 rpm (revolution per minute) for 60 seconds, followed by soft baking for another 60 seconds on the hot plate at 100°C. A laser writer (Heidelberg  $\mu\text{PG}$  101) was used to pattern the hole array design (L-Edit) on the photoresist-coated  $\text{Al}_2\text{O}_3$  on CdTe.

We performed a series of control experiments to optimize the laser dose that could polymerize the photoresist on a rough surface CdTe while maintaining the size of the array of the design [19]. We found a relatively high beam energy (an effective dose of 13.5 mW) is needed for CdTe compared to traditional Si flat samples (10 mW). The photoresist was developed in a solution (AZ Developer 1:1) for 60 seconds and soaked in DI water. We used another solution (AZ 300 MIF) to selectively etch the exposed  $\text{Al}_2\text{O}_3$  on CdTe after the photoresist development. This chemical contains a small amount of tetramethyl ammonium hydroxide (< 3 % TMAH), which has a faster etch rate for  $\text{Al}_2\text{O}_3$  than photoresist. The  $\text{Al}_2\text{O}_3$  etching was conducted for 20 minutes, followed by the photoresist removal and cleaning using acetone, IPA, deionized water, and  $\text{N}_2$ -blown dried.

The metal contact for each device was designed to be 2 mm  $\times$  2 mm in size. We fabricated a shadow mask using a stainless-

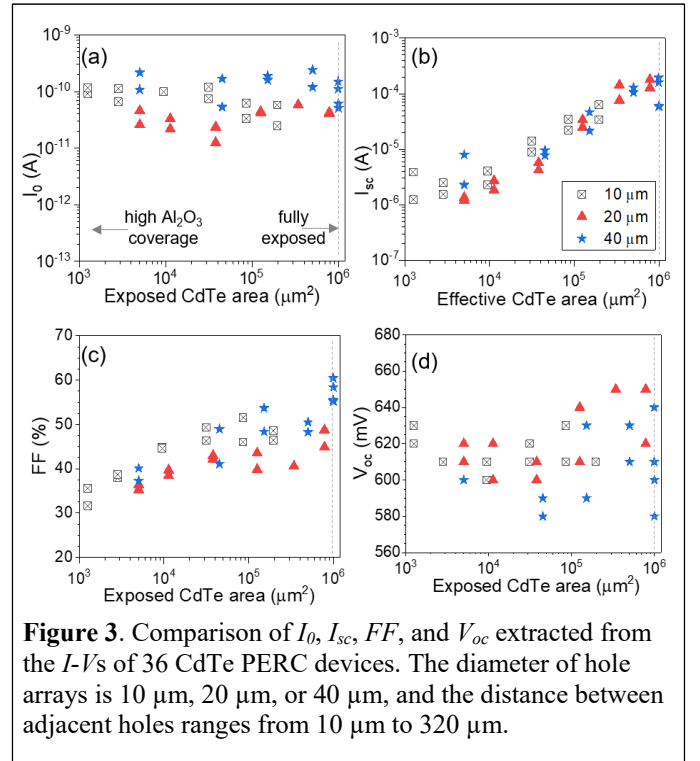
steel foil (40  $\mu\text{m}$ ) containing a square array (3  $\times$  4) with a spacing of 1 mm. This shadow mask was aligned to the hole array patterns on  $\text{Al}_2\text{O}_3/\text{CdTe}$  (top right in Figure 2). The sample was placed on a holder in an electron beam evaporator. Thin films of Cu/Au (3 nm/80 nm) were deposited on the patterned  $\text{Al}_2\text{O}_3/\text{CdTe}$  through the shadow mask, which served as a back contact. A front indium contact was formed on TCO after removing the CdTe segment using a razor blade. Figure 2 displays the complete CdTe PERC devices.

The dark and light current-voltage characteristics were measured using a probe station (dark enclosure) connected to a semiconductor analyzer (Agilent 4145C). Each probe tip (25  $\mu\text{m}$  diameter W-tip) was placed on top and bottom metal contact while recording the  $I$ - $V$ s using the LabVIEW program. Before the measurements, the solar simulator (G2V) was calibrated to 1-sun using a reference cell (Newport; 91150V).

### III. RESULTS AND DISCUSSION

We analyze the dark and light  $I$ - $V$ s measured from 36 CdTe PERC devices having various hole array patterns. All devices consisted of a patterned area in the center (1 mm  $\times$  1 mm) of the metal contact (2 mm  $\times$  2 mm). For a statistical comparison, we estimate the exposed CdTe area of each device from the design, where the Cu/Au metal is directly deposited on CdTe without the  $\text{Al}_2\text{O}_3$  layer. Figure 3 summarizes the parameters ( $I_0$ ,  $I_{sc}$ ,  $FF$ , and  $V_{oc}$ ) of CdTe PERC.

The distribution of leakage current of our devices (Figure 3a) is relatively constant, supporting the fidelity of the fabrication processes developed in this work. The magnitudes of  $I_{sc}$  and  $FF$



proportionally increase with the exposed CdTe area. As seen in Figure 3(b), the  $I_{sc}$  of the CdTe PERC having an exposed CdTe area of 1 % is 1  $\mu\text{A}$ . This current increases to 10 mA when the  $\text{Al}_2\text{O}_3$  layer is fully removed in the patterned area (1 mm  $\times$  1 mm). The  $FF$  increases to a factor of two (approximately 30 % to 60 %) with the  $\text{Al}_2\text{O}_3$  removal. These trends are expected as the electrically resistive  $\text{Al}_2\text{O}_3$  layer (20 nm thick) can interfere with the photocarrier collection (hole carriers) from CdTe to metal contact.

Interestingly, the  $V_{oc}$  trend (Figure 3d) for the As-doped CdTe PERC is notably different from that of  $I_{sc}$  and  $FF$ . The  $V_{oc}$  ranges from 580 mV to 660 mV, which seems independent to the exposed CdTe areas. In a close look, the  $V_{oc}$  slightly decreases from  $\approx 640$  mV to  $\approx 590$  mV when the CdTe area increases from  $10^3 \mu\text{m}^2$  (1 % of the total device area) to  $10^4 \mu\text{m}^2$  (10 %). The  $V_{oc}$  increases as high as 660 mV with the increase of the exposed CdTe area (40 %  $\sim$  80 %). The  $V_{oc}$  of the control devices, which have the fully open CdTe area (100 %), ranges from 580 mV to 640 mV, still below the highest  $V_{oc}$  observed with the patterned  $\text{Al}_2\text{O}_3$  PERC devices. We note that the  $V_{oc}$  trend of As-doped PERC is also significantly different from our Cu-doped CdTe PERC, where the  $V_{oc}$  decreases with the increased CdTe exposed area (not shown in the data). Our results indicate the electrically-active  $\text{Al}_2\text{O}_3$  patterns could play

an important role in determining the  $V_{oc}$  of advanced CdTe-based solar cells.

We have examined the performance of the As-doped CdTe PERC solar cells under heating. We annealed the complete PERC devices at 70  $^\circ\text{C}$  for 2.5 hours in this preliminary experiment. The diameter of the patterned  $\text{Al}_2\text{O}_3$  is 10  $\mu\text{m}$ , and the adjacent hole distance ranges from 10  $\mu\text{m}$  to 320  $\mu\text{m}$ . Figures 4 (a, b) shows the light  $I$ - $V$ s collected “before” and “after” the heating. Overall, the PERC devices preserve good diode behaviors after the heating.

Figures 4 (c  $\sim$  f) compare the device parameters of the saturation current ( $I_s$ ),  $I_{sc}$ ,  $FF$ , and  $V_{oc}$  extracted from the  $I$ - $V$ s. The magnitudes of the  $I_s$  and  $V_{oc}$  are relatively constant, while the  $I_{sc}$  and  $FF$  increase with the exposed CdTe area, with similar trends observed in Figure 3. The magnitudes of  $I_s$ ,  $I_{sc}$ , and  $FF$  show only slight variation after the heating at 70  $^\circ\text{C}$ . In contrast, the  $V_{oc}$  of the CdTe PERC increases after annealing with a magnitude as high as  $\approx 10$  % of its initial value (e.g., 600 mV to 650 mV). Presumably, the group-V dopant (As) in the CdTe bulk could be more activated, or the defects near  $\text{Al}_2\text{O}_3$  may be further passivated during the annealing [20]. Further studies are in progress to gain a better understanding of such heating effects and back-contact passivation.

#### IV. CONCLUSIONS

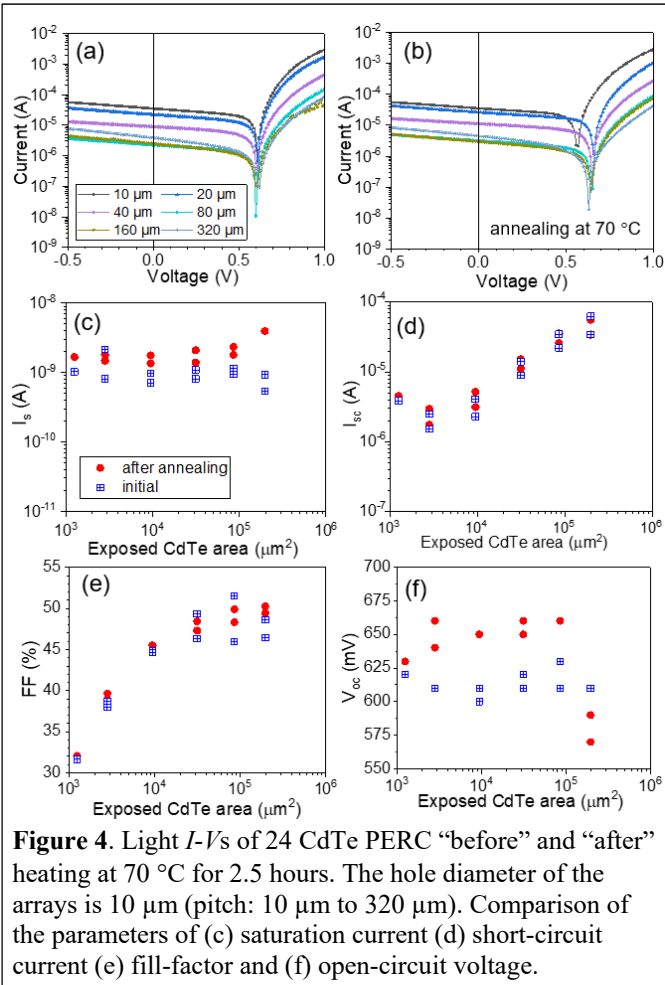
In summary, we have demonstrated the fabrication of CdTe PERC solar cells with a patterned  $\text{Al}_2\text{O}_3$  passivation layer. Our process based on laser-beam lithography enables reproducible patterning on a rough surface CdTe while maintaining the size of the array in the design. Quantitative analysis of the As-doped CdTe PERC shows a proportional increase of  $FF$  and  $J_{sc}$  with an exposed CdTe area. We have observed that the complete CdTe PERC annealing increases the  $V_{oc}$  by  $\approx 10$  % of their initial magnitudes, whereas the  $I_s$ ,  $I_{sc}$ , and  $FF$  show negligible changes. Our results indicate that the subsurface electronic properties of CdTe and the interplay between carrier selectivity and collection of the patterned  $\text{Al}_2\text{O}_3$  could be responsible for the observed PV characteristics.

#### ACKNOWLEDGEMENT

The authors thank B. Baker, A. Hurlbut, P. Perez, D. Albin, A. Chowdhury, and D. Maggini for experimental assistance and valuable discussions in this work. This research was supported by the U.S. Department of Energy’s Office of Energy Efficiency and Renewable Energy (EERE) under the DE-FOA-0002064 program award number DE-EE0008983. We acknowledge support in part by the National Science Foundation (NSF) CAREER Award No. 2048152.

#### REFERENCES

- [1] G. M. Wilson *et al.*, “The 2020 photovoltaic technologies roadmap,” (in English), *Journal of Physics D-Applied Physics*, vol. 53, no. 49, Dec 2 2020.



- [2] “Cadmium Telluride,” Energy.gov. <https://www.energy.gov/eere/solar/cadmium-telluride> (accessed Oct. 10, 2022).
- [3] K. J. Hsiao and J. R. Sites, “Electron reflector to enhance photovoltaic efficiency: Application to thin-film CdTe solar cells,” *Progress Photovolt., Res. Appl.*, vol. 20, no. 4, pp. 486–489, 2012
- [4] G. K. Liyanage, A. B. Phillips, F. K. Alfadhili, R. J. Ellingson, and M. J. Heben, “The Role of Back Buffer Layers and Absorber Properties for >25% Efficient CdTe Solar Cells,” *ACS Appl. Energy Mater.*, vol. 2, no. 8, pp. 5419–5426, Aug. 2019, doi: 10.1021/acsaem.9b00367.
- [5] A. Kanevce and T. Gessert, “Optimizing CdTe solar cell performance: Impact of variations in minority-carrier lifetime and carrier density profile,” *IEEE J. Photovolt.*, vol. 1, no. 1, pp. 99–103, Jul. 2011.
- [6] Kuciauskas, D.; Moseley, J.; Šč ajev, P.; Albin, D. Radiative Efficiency and Charge-Carrier Lifetimes and Diffusion Length in Polycrystalline CdSeTe Heterostructures. *Phys. Status Solidi RRL* 2020, 14, No. 1900606.
- [7] L. Wu et al., “CdTe surface passivation by electric field induced at the metal-oxide/CdTe interface,” *Solar Energy*, vol. 225, pp. 83–90, Sep. 2021, doi: 10.1016/j.solener.2021.07.015.
- [8] Li, X., Shen, K., Li, Q., Deng, Y., Zhu, P., Wang, D., 2018b. “Roll-over behavior in current-voltage curve introduced by an energy barrier at the front contact in thin film CdTe solar cell,” *Sol. Energy* 165, 27–34.
- [9] M. A. Green, A. W. Blakers, and J. Shi, “19.1% efficient silicon solar cell,” *Appl. Phys. Lett.* 44 (1984) 1163-1164.
- [10] A.W. Blakers, A. Wang, A.M. Milne, J. Zhao, M.A. Green, “22.8% Efficient Silicon Solar Cell,” *Appl. Phys. Lett.* 55 (1989) 1363–1365.
- [11] J. M. Kephart et al., “Sputter-Deposited Oxides for Interface Passivation of CdTe Photovoltaics,” *IEEE J. Photovoltaics*, vol. 8, no. 2, pp. 587–593, Mar. 2018, doi: 10.1109/JPHOTOV.2017.2787021.
- [12] J. Liang et al., “Rectification and tunneling effects enabled by Al<sub>2</sub>O<sub>3</sub> atomic layer deposited on back contact of CdTe solar cells,” *Appl. Phys. Lett.*, vol. 107, no. 1, p. 013907, Jul. 2015, doi: 10.1063/1.4926601.
- [13] F. K. Alfadhili et al., “Back-Surface Passivation of CdTe Solar Cells Using Solution-Processed Oxidized Aluminum,” *ACS Appl. Mater. Interfaces*, vol. 12, no. 46, pp. 51337–51343, Nov. 2020, doi: 10.1021/acsaami.0c12800.
- [14] Y. Su et al., “Band Alignment for Rectification and Tunneling Effects in Al<sub>2</sub>O<sub>3</sub> Atomic-Layer-Deposited on Back Contact for CdTe Solar Cell,” *ACS Appl. Mater. Interfaces*, vol. 8, no. 41, pp. 28143–28148, Oct. 2016, doi: 10.1021/acsaami.6b07421.
- [15] A. Kanevce, M. O. Reese, T. M. Barnes, S. A. Jensen, and W. K. Metzger, “The roles of carrier concentration and interface, bulk, and grain-boundary recombination for 25% efficient CdTe solar cells,” *Journal of Applied Physics*, vol. 121, no. 21, p. 214506, Jun. 2017, doi: [10.1063/1.4984320](https://doi.org/10.1063/1.4984320).
- [16] D. Kuciauskas, J. M. Kephart, J. Moseley, W. K. Metzger, W. S. Sampath, and P. Dippo, “Recombination velocity less than 100 cm/s at polycrystalline Al<sub>2</sub>O<sub>3</sub>/CdSeTe interfaces,” *Appl. Phys. Lett.*, vol. 112, no. 26, p. 263901, Jun. 2018, doi: 10.1063/1.5030870.
- [17] Q. Lin et al., “A novel p-type and metallic dual-functional Cu–Al<sub>2</sub>O<sub>3</sub> ultra-thin layer as the back electrode enabling high performance of thin film solar cells,” *Chem. Commun.*, vol. 52, no. 71, pp. 10708–10711, 2016, doi: 10.1039/C6CC04299F.
- [18] A. H. Munshi, A. H. Danielson, A. Kindvall, K. Barth, and W. Sampath, “Investigation of Sputtered Oxides and p+ Back-contact for Polycrystalline CdTe and CdSeTe Photovoltaics,” in 2018 IEEE 7th World Conference on Photovoltaic Energy Conversion (WCPEC) (A Joint Conference of 45th IEEE PVSC, 28th PVSEC & 34th EU PVSEC), Jun. 2018, pp. 3009–3012. doi: 10.1109/PVSC.2018.8548203.
- [19] K. M. Powell, Y.-L. Hsu, E. K. Roy, D. J. Magginiti, and H. P. Yoon, “Fabrication of Microscale Back-Contact Arrays for Local Charge Transport Measurements,” in *2022 IEEE 49th Photovoltaics Specialists Conference (PVSC)*, Philadelphia, PA, USA, Jun. 2022, pp. 1–4. doi: [10.1109/PVSC48317.2022.9938877](https://doi.org/10.1109/PVSC48317.2022.9938877).
- [20] D. J. Elliott, “Annealing and Planarizing,” in *Ultraviolet Laser Technology and Applications*, Elsevier, 1995, pp. 209–250. doi: [10.1016/B978-0-12-237070-0.50011-X](https://doi.org/10.1016/B978-0-12-237070-0.50011-X).